



# Micromechanical cantilever resonators with integrated optical interrogation

M. Hoffmann, H. Bezzaoui, E. Voges

Lehrstuhl für Hochfrequenztechnik, Universität Dortmund, D-44221 Dortmund, Germany

Received 14 July 1993; accepted in revised form 3 January 1994

#### Abstract

The combination of integrated optics and micromechanics on silicon offers micromechanical devices with optical read-out. Integrated optical waveguide devices with silicon oxinitride (SiON) strip waveguides are fabricated by CMOS-compatible PECVD and RIE processes. The stress-compensated  $SiO_2/SiON/SiO_2$  waveguide layer system is utilized to fabricate cantilever resonators with 50-200 kHz resonance frequency, and a quality factor of about 100. The coupling between optical waveguides across 2  $\mu$ m gaps is employed to detect resonator vibrations. Arrays of eight resonators with 10 and 1 kHz frequency spacings which are connected via  $1 \times 8$  waveguide branching structures have been fabricated and tested.

#### 1. Introduction

Silicon technology enables complex sensor microsystems to be fabricated by a monolithic integration of micromechanical devices with integrated optical circuits, photodiodes and CMOS microelectronics for signal detection and processing. When combining only micromechanics and integrated optics [1–7], one can realize micromechanical sensor systems with optical read-out. Optical sensor interrogation by integrated optical waveguide devices avoids the adjustment and stability problems of hybrid optical techniques [8,9]. The additional integration of photodiodes [5,6] and CMOS microelectronics [10] yields intelligent sensor systems with integrated signal processing.

The integrated optical waveguide devices are fabricated by CMOS-compatible low-temperature (350 °C) plasma deposition (PECVD) of oxynitride (SiON) and SiO<sub>2</sub> layers on thermally oxidized silicon substrates, and a delineation of optical strip waveguides by reactive ion etching (RIE).

Silicon-based micromechanical devices can be fabricated by standard anisotropic etching or RIE. Here, we take advantage of the excellent mechanical properties of the SiO<sub>2</sub>/SiON/SiO<sub>2</sub> waveguide multilayer to fabricate membranes, micro beams or bridges and cantilever resonators [1,4,5,7].

We demonstrate the integration technique by optically interrogated cantilever resonator arrays.

# 2. Waveguide and micromechanical device technologies

Single-mode strip waveguides for 0.633  $\mu$ m and 0.8  $\mu$ m wavelengths are fabricated by PEVCD of silicon oxynitride (SiON) and SiO<sub>2</sub> layers on thermally oxidized silicon, and a delineation of the stripes by RIE [1].

The insert in Fig. 1 depicts the waveguide geometry and the waveguide parameters. A low refractive index (n=1.52) of the SiON layer was chosen for a high reproducibility and yield. In addition, the indicated parameters yield stress-compensated  $SiO_2/SiON/SiO_2$  layers. At 0.633-0.8  $\mu$ m wavelength, the waveguides exhibit low losses (below 0.25 dB/cm for TE-polarization), determined from the finesse of ring resonators. Moreover, the strong field confinement with about 1  $\mu$ m vertical field width and about 3  $\mu$ m lateral field width allows small bending radii down to 500  $\mu$ m. This yields a relatively high package density of optical devices such as Y-branches, directional couplers or Mach-Zehnder interferometers.

Micromechanical elements such as membranes, micro bridges and cantilevers are fabricated with stress-compensated SiO<sub>2</sub>/SiON/SiO<sub>2</sub> dielectric sandwiches.

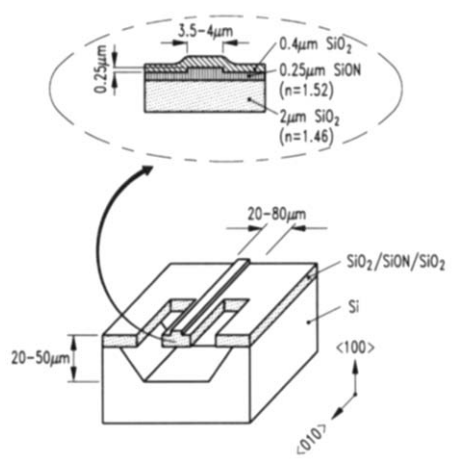


Fig. 1. Scheme of an SiO<sub>2</sub>/SiON/SiO<sub>2</sub> cantilever with integrated optical strip waveguide.

Fig. 1 shows the configuration of a cantilever fabricated by anisotropic silicon etching. For  $\langle 100 \rangle$  oriented wafers the corresponding photomask was aligned at 45° to the wafer flat in order to employ the high etch rates of  $\langle 100 \rangle$  and  $\langle 110 \rangle$  planes [11].

The application of standard KOH etching, however, degrades the PECVD layers due to their non-stoichiometric composition, resulting in enhanced optical losses. In addition, the stress and refractive index of the SiO<sub>2</sub> increased due to potassium indifussion. Therefore, we utilized NH<sub>4</sub>OH-H<sub>2</sub>O<sub>2</sub>-H<sub>2</sub>O (AHW) [12] for anisotropic etching.

AHW etching results in an increased surface roughness, particularly for the 'bottom' surface, in comparison to KOH etching. This is, however, of minor importance when utilizing the dielectric sandwich layer for micromechanical devices. AHW allows the etching of silicon with a high selectivity to SiO<sub>2</sub>, and, if a small amount of silicon (0.1 g/l) is added to the etchant, to aluminium [12]. This fact and the absence of metal ions yield a CMOS-compatible etching process.

# 3. Cantilever resonator with optical read-out

Cantilever resonators with optical interrogation are fabricated according to the scheme of Fig. 1. The SEM photo in Fig. 2 shows an SiO<sub>2</sub>/SiON/SiO<sub>2</sub> cantilever resonator with integrated optical waveguides. The variation of the optical coupling across the gap is employed for vibration detection. With optimized RIE process parameters (20 sccm CHF<sub>3</sub>, 2.5 sccm O<sub>2</sub>, 30 mTorr, 80 W), a high sidewall quality is achieved with only 3 dB optical coupling loss for a 2  $\mu$ m gap. In contrast to silicon-based cantilevers, distortions of the optical signal due to reflections of silicon sidewalls are negligible here.

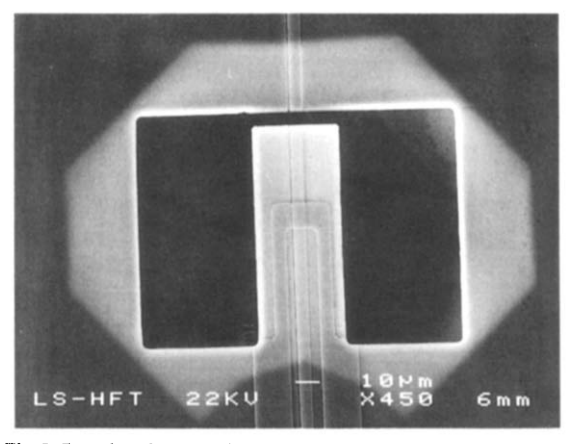


Fig. 2. Scanning electron microscope (SEM) photograph of an SiO<sub>2</sub>/SiON/SiO<sub>2</sub> cantilever resonator with optical waveguide, 4 μm gap width and thermal excitation by a U-shaped Al heating electrode.

The cantilever vibrations can be induced by mechanical or electrical forces [13]. In addition, optically [14] or electrically [15] applied thermal power leads to a cantilever deflection, which is essentially due to thermally induced stress effects, and the 'bimetal effect' caused by different thermal expansion coefficients between the metal electrode and the SiO<sub>2</sub> cantilever.

For test purposes we utilized electrical heating with the aid of U-shaped electrodes as shown in Fig. 2. This type of excitation is easily implemented by planar technologies. It yields a modulation bandwidth beyond 300 kHz.

The mechanical resonance frequency of the cantilever is influenced by its length L and its thickness d. Vibrational mechanics [16] yields cantilever resonance frequencies

$$f_i = \left(\frac{E}{12\sigma}\right)^{1/2} \frac{d}{L^2} M_i^2 \tag{1}$$

where E is Young's modulus (we insert  $E=6.7\times10^{10}$  N/m² for thin SiO<sub>2</sub> layers [17]) and  $\sigma$  is the specific mass ( $\sigma$ =2200 kg/m³ for SiO<sub>2</sub> [17]). The coefficients  $M_i$  with  $M_1$ =1.875,  $M_2$ =4.694,  $M_3$ =7.855 correspond to the vibrational modes. The fundamental vibrational mode (one node) with  $M_1$  has an almost parabolic shape of the deflected cantilever. In Eq. (1) we used the simple formula  $I_{zz}=d^3w/12$  for the appropriate moment of inertia of the cantilever with a width w. Improved results for  $I_{zz}$ , which take account of the rib waveguide structure, can be obtained from the parallel axes theorem [18].

One should note that the resonance frequency does not depend on the cantilever width w. This also holds when taking the rib waveguide into account, if the ratio of its width and w is kept constant. Resonance frequencies in the 100 kHz range are easily achieved.

The resonance frequency  $f_1$  of the fabricated cantilevers deviated from the theoretical values by typically 5%. These deviations are mainly due to the unknown E value of the sandwich layer, the neglect of its internal stresses and the inaccuracies of the fabricated cantilever thickness d.

Fig. 3 shows the optically detected resonance frequency  $f_1$  of  $SiO_2/SiON/SiO_2$  cantilevers as a function of the cantilever length L, and the theoretical values obtained from Eq. (1). The quality factor Q of the resonator is measured by determining the  $\pm 45^\circ$  phase off-set frequencies  $f_r$  of the coupled optical signal in comparison to the phase at resonance  $(f_1)$  under low drive-power conditions.

The evaluation of

$$Q = \frac{f_1}{f_r(+45^\circ) - f_r(-45^\circ)}$$
 (2)

yields quality factors of 125 for cantilevers with length  $L=160~\mu m$ . This value is far above the quality factor  $Q\approx 15$  [13] for thin SiO<sub>2</sub> cantilevers. The quality factor of our cantilever resonators is mainly determined by air damping. It may be considerably increased for cantilevers under vacuum conditions [13].

The guided field distribution of the SiO<sub>2</sub>/SiON/SiO<sub>2</sub> strip waveguides is to a good approximation given by Gaussian field distributions in the lateral and vertical directions. This Gaussian field excites a Gaussian beam at the waveguide front faces (Fig. 4). (This is strictly true within the Fresnel approximation of the wave

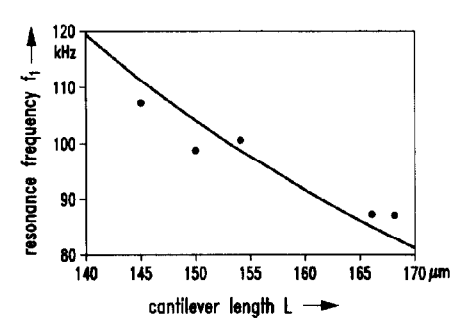


Fig. 3. Resonance frequency  $f_1$  of SiO<sub>2</sub>/SiON/SiO<sub>2</sub> cantilevers as a function of length L. The solid line indicates theoretical values from Eq. (1). The dots represent experimental values for the parameters of Fig. 1.

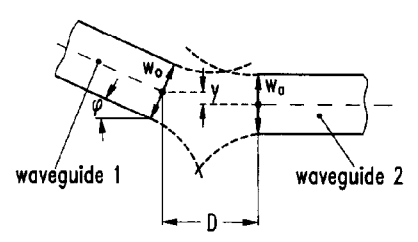


Fig. 4. Overlap of Gaussian beams for off-set strip waveguides (vertical off-set y, waveguide separation D, angular displacement  $\varphi$ ).

equations [19].) The power coupling coefficient K between two off-set strip waveguides is then calculated from the normalized overlap integral of both Gaussian beams (Fig. 2) [19]. This yields for small angular displacements,  $j \ll 1$ , a power coupling with

$$K = \frac{2}{(4 + Z_x^2)^{1/2}} \frac{2}{(4 + Z^2)^{1/2}} \times \exp\left\{\frac{2}{4 + Z^2} \left[ -2 \frac{y^2}{w_0^2} - \Phi^2(2 + Z^2) + 2 \frac{y}{w_0} \Phi Z \right] \right\}$$
(3)

The parameters

$$Z = D\lambda_0/\pi w_0^2, \quad Z_x = D\lambda_0/\pi w_x^2 \tag{4}$$

with the gap-width D, the free-space wavelength  $\lambda_0$  and the  $1/e^2$  intensity width  $w_0$  of the guided mode in vertical direction and  $w_x$  in the lateral direction determine the influence of the gap.

For the vertical deflection y we insert a sinusoidal modulation with

$$y = y_0 + \hat{y} \sin(\omega t) \tag{5}$$

at the modulation radian frequency ω.

The function

$$\Phi = -\frac{\pi w_0}{\lambda_0} \varphi = -\frac{\pi w_0}{\lambda_0} \arctan\left(\frac{2y}{L}\right)$$
 (6)

contains the angular displacement. (On the right-hand side of Eq. (6) we inserted a parabolic shape for the deflected cantilever.)

For a cantilever length  $L \gg |y_0 + \hat{y}|$  the contribution of the angular misalignment may be neglected. Then, we have a simple Gaussion function for the power coupling as a function of the cantilever deflection y.

Fig. 5(a) shows the variation of the power coupling with cantilever deflection y for  $\lambda_0 = 0.633 \,\mu\text{m}$  wavelength, a field width  $w_0 = 0.8 \,\mu\text{m}$ , cantilever length  $L = 200 \,\mu\text{m}$  and gap width  $D = 2 \,\mu\text{m}$ .

We observed from Fig. 5(a) that submicron deflections can be detected optically. The time dependence of the coupled power for a sinusoidal modulation in Fig. 5(b) exhibits sharp peaks for a resonance excitation with large deflection amplitudes.

The above calculations are in close agreement with experimental results. This is demonstrated in Fig. 6 by the example of a resonance excitation of a cantilever resonator (experimental parameters:  $L=150~\mu m$ ,  $P_{\rm excit}=50~{\rm mW}$ ).

#### 4. Optically connected resonator arrays

Planar technologies readily allow the fabrication of optically connected resonator arrays. Fig. 7 shows the

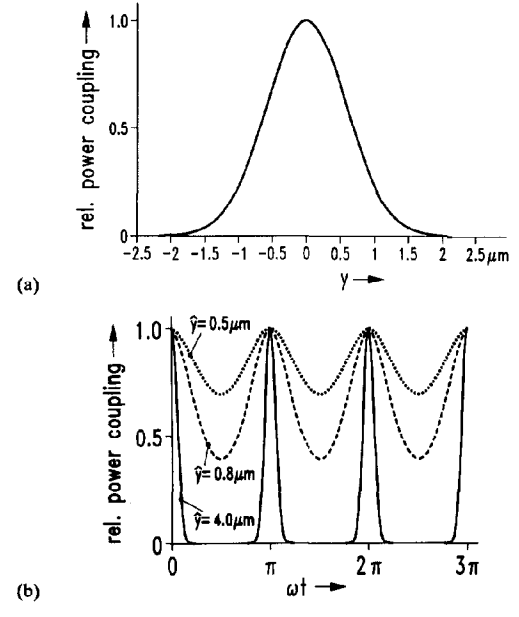


Fig. 5. (a) Normalized power coupling as a function of the cantilever deflection y. (b) Time dependence of the power coupling for a sinusoidal modulation with  $y=\hat{y}$  sin  $\omega t$  and different amplitudes  $\hat{y}$  ( $\lambda=0.633~\mu m$ ,  $w_0=0.8~\mu m$ ,  $L=200~\mu m$ ,  $D=2~\mu m$ ).

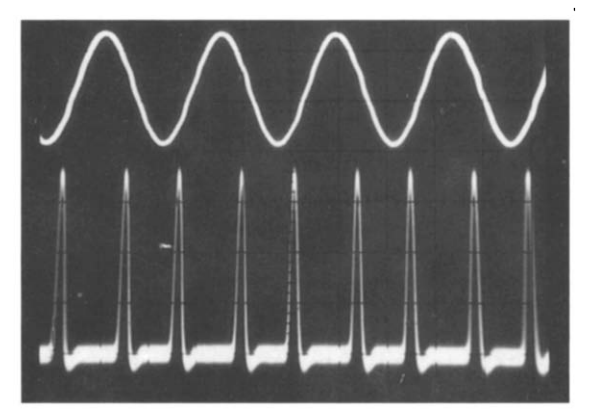


Fig. 6. Driving signal (upper trace) and detector signal (lower trace) for a large-amplitude resonance excitation of a cantilever resonator ( $\lambda = 0.633 \, \mu \text{m}$ ,  $w_0 = 0.8 \, \mu \text{m}$ ,  $L = 150 \, \mu \text{m}$ ,  $f \approx 90 \, \text{kHz}$ ).

scheme of an array with eight cantilever resonators with different resonance frequencies. Experimentally, we realized resonator arrays with a 20 kHz frequency spacing ( $f_{\rm min}=85$  kHz,  $f_{\rm max}=205$  kHz), a 10 kHz spacing ( $f_{\rm min}=30$  kHz,  $f_{\rm max}=100$  kHz) and a 1 kHz spacing ( $f_{\rm min}=96$  kHz,  $f_{\rm max}=103$  kHz). The optical input signal is fed to the cantilevers by a branching network built up with cascaded Y-junctions. The dimensions of the branching network are 10 mm length and 2 mm width. For fibre coupling we utilized polarization-maintaining fibres (York HB 800), which are glued to the chip endface by UV-curing epoxy. Typical coupling losses are between 3 and 5 dB. Fig. 8 shows a scattered light

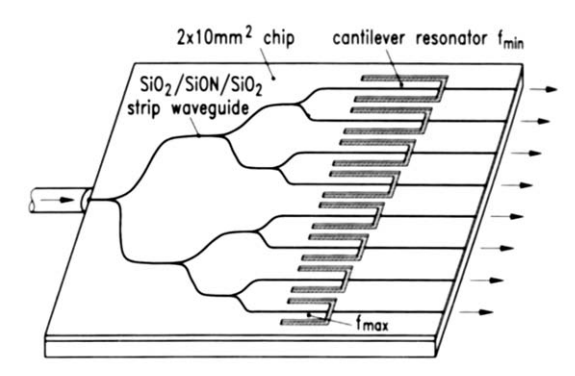


Fig. 7. Array of cantilever resonators with different resonance frequencies and integrated optical branching structure for optical readout.

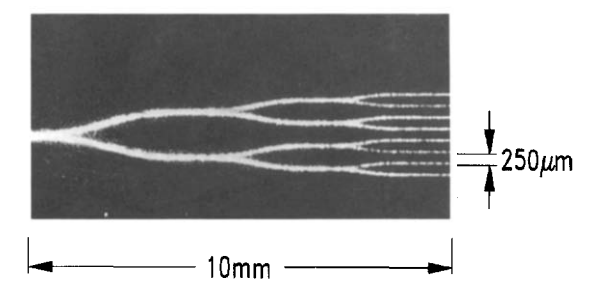


Fig. 8. Scattered light photograph of the light distribution ( $\lambda = 0.633$   $\mu$ m) within the  $1\times8$  optical branching network.

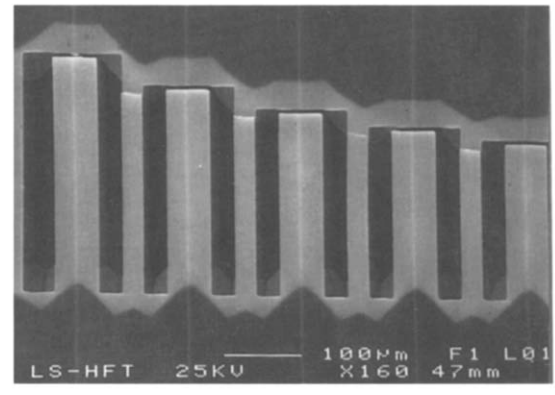


Fig. 9. SEM photograph of a cantilever resonator array with 20 kHz frequency spacing of the resonance frequencies.

photograph of the branching network, and demonstrates the low losses of the Y-junctions and the low bending losses.

The spacing of the resonance frequencies of the cantilevers is realized by their different lengths L (see Fig. 9). Prescribed values could be accurately realized.

#### 5. Conclusions

The optical interrogation of silicon-based micromechanical devices with the aid of integrated optical waveguides has been demonstrated for cantilever resonators. Arrays of eight cantilever resonators have been connected by integrated branching devices. The experimental cantilever resonance frequencies in the range 50-200 kHz agree well with the theoretical values. A quality factor of about 100 was determined. The butt coupling of the thermally driven cantilevers has been both simulated and measured. Both results are in a good agreement.

The application of planar technologies for combined optical and mechanical systems is particularly attractive for the fabrication of sensor arrays with optical readout.

### Acknowledgement

This work has been supported by BMFT (Bundesministerium für Forschung und Technologie).

# References

- H. Bezzaoui and E. Voges, Integrated optics combined with micromechanics on silicon, Sensors and Actuators A, 29 (1991) 219-223.
- [2] S. Wu and H.J. Frankena, Micro-mechanical structures as integrated optical sensor elements, *Tech. Digest, Integrated Photonic Research Topical Meeting, New Orleans, LA, USA, April 1992*, pp. 158-159.
- [3] K.E. Burcham, G.N. DeBrabander and J.T. Boyd, Micromachined silicon cantilever beam accelerometer incorporating an integrated optical waveguide, SPIE Proc., Vol. 1793, SPIE Symp. OE/Fibers '92, Boston, MA, USA, Sept. 1992, Paper 1793-10.
- [4] H. Bazzaoui, M. Hoffmann and E. Voges, Micromechanical devices on silicon with integrated optical read-out, in H. Reichl (ed.), Micro System Technologies '92, VDE-Verlag, Berlin, 1992, pp. 234-251.
- [5] J. Müller, D. Zurhelle, K. Fischer, A. Löffler-Peters and R. Hoffmann, Integrated optical pressure sensor with coupling structures, SPIE Proc., Vol. 1794, SPIE Symp. OE/ Fibers '92, Boston, MA, USA, Sept. 1992, Paper 1794-17.
- [6] K. Fischer, D. Zurhelle, R. Hoffmann, F. Wasse and J. Müller, Fully integrated optical force and pressure sensor based on SiON layers, Proc. Eur. Conf. Integrated Optics, ECIO 93, Neuchâtel, Switzerland, Apr. 1993, pp. 12/7-12/9.
- [7] E. Voges, H. Bezzaoui and M. Hoffmann, Integrated optics and microstructures on silicon, Proc. Eur. Conf. Integrated Optics, ECIO 93, Neuchâtel, Switzerland, Apr. 1993, pp. 12/ 4-12/6.
- [8] N.A.D. Stockes, R.M.A. Fatah and S. Vankatesh, Selfexcitation in fibre-optic microresonator sensors, Sensors and Actuators, A21-A23 (1990) 369-372.
- [9] G. Grosch, Hybrid fiber-optic/micromechanical frequency encoding displacement sensor, Sensors and Actuators, A21-A23 (1990) 1128-1131.
- [10] U. Hilleringmann, K. Knospe, C. Heite, K. Schumacher and K. Goser, A silicon based technology for monolithic integration of waveguides and VLSI CMOS circuits, Microelectron. Eng., 15 (1991) 289-293.
- [11] A. Heuberger, Mikromechanik, Springer, Berlin, 1989, p. 139.

- [12] U. Schnackenberg, W. Benecke and B. Löckel, NH₄OH-based etchants for silicon micromachining: influence of additives and stability of passivation layers, Sensors and Actuators A, 25-27 (1991) 1-7.
- [13] K.E. Petersen, Dynamic micromechanics on silicon: techniques and devices, *IEEE Trans. Electron Devices*, ED-25 (1978) 1241-1250.
- [14] D. Walsh and B. Culsahw, Optically activated silicon microresonator transducer: an assessment on material properties, Sensors and Actuators A, 25-27 (1991) 711-716.
- [15] T.S.J. Lammerink, M. Elwenspoek and J.H.J. Fluitman, Frequency dependence of thermal excitation of micromechanical resonators, Sensors and Actuators A, 25-27 (1991) 685-689.
- [16] L. Meirovitch, Elements of Vibration Analysis, McGraw-Hill, New York, 1975, p. 211.
- [17] K.E. Petersen and C.R. Guarnieri, Young's modulus measurement of thin films using micromechanics, J. Appl. Phys., 50 (1979) 6761-6766.
- [18] W. Flügge, Handbook of Engineering Mechanics, McGraw-Hill, New York, 1st edn., 1962, p. 5-2.
- [19] J.A. Arnaud, Beam and Fiber Optics, Academic Press, London, 1976.

# **Biographies**

Martin Hoffmann was born in Hemer, Germany, on October 3, 1966. He received the Dipl.-Ing. degree in electrotechnics from the University of Dortmund, Germany, in January 1992. Since 1992 he has been an assistant at the Lehrstuhl für Hochfrequenztechnik at the University of Dortmund, where he is engaged in investigations on integrated optics on silicon. His current interests are waveguides for 1.3/1.5 μm wavelength.

Hocine Bezzaoui was born in Tizi-Ouzou, Algeria, on November 1, 1954. He received the Dipl.-Ing. degree in electrotechnics from the University of Dortmund, Germany, in November 1988. Since 1989 he has been an assistant at the Lehrstuhl für Hochfrequenztechnik at the University of Dortmund, where he is engaged in investigations on integrated optics on silicon. In 1992 he received the Doktor-Ingenieur degree from the Universität Dortmund. His current interests are in integrated optical/micromechanical sensors.

Edgar Voges was born in Braunschweig, Germany, on August 26, 1941. He received the Diplom-Physiker degree in physics and the Doctor-Ingenieur degree from the Technische Universität Braunschweig, Germany, in 1967 and 1970, respectively. From 1967 to 1974 he was an assistant at the Institut für Hochfrequenztechnik of the University of Braunschweig. From 1974 to 1977 he was professor at the Department of Electrical Engineering of the University of Dortmund. From 1977 to 1982 he was professor of communication engineering at the Fernuniversität, Hagen, Germany. In 1982 he rejoined the Department of Electrical Engineering of the University of Dortmund, Lehrstuhl für Hochfrequenztechnik. His current interests are in optical communications, integrated optics and high-frequency integrated circuits.